Accurate analysis of ellipsometric data for thick transparent films

Yuan Zhao(赵 源)[1,2], Mingyu Sheng(盛明裕)[1,3], Yuxiang Zheng(郑玉祥)[1], and Liangyao Chen(陈良尧)[1*]

[1]*Department of Optical Science and Engineering, Fudan University, Shanghai 200433, China*
[2]*Department of Optical Electronics Information Engineering, Shanghai Second Polytechnic University, Shanghai 201209, China*
[3]*Department of Electronics Information Engineering, Shanghai Business School, Shanghai 200235, China*
[*]*Corresponding author: lychen@fudan.ac.cn*

Received September 26, 2010; accepted December 10, 2010; posted online April 18, 2011

Using e-beam evaporation, the ellipsometric parameters of thick transparent films are studied with the modified analysis method for the SiO_2 film samples deposited onto the Si substrate. The ellipsometric parameters are measured at the incidence angles changing from 50° to 70° and in the 3–4.5 eV photon energy range. The error in the conventional method can be significantly reduced by the modified ellipsometric method considering the spatial effect to show good agreement between the theoretical and experimental results. The new method presented in this letter can be applied to other optical measurement of the periodic or non-periodic film structures.

OCIS codes: 310.6860, 260.2130.
doi: 10.3788/COL201109.053101.

Spectroscopic ellipsometry is widely used as an effective and nondestructive optical technique to determine physical parameters of film structures, such as refractive index, extinction coefficient, physical thickness, and so on[1−9]. Spectroscopic ellipsometry typically measures the change of polarization between the incident and reflected electromagnetic waves interacting on the sample. The polarization state is determined by the direct measurement of the ratio of the complex reflection coefficients (magnitude and phase) of two orthogonal linear polarizations at a particular angle of incidence.

Thick transparent film, such as the SiO_2 film deposited on the Si substrate with the film thicker than the incident wavelength, can be applied in various fields, such as microelectronics, micromechanics, integrated optics, and so on. Spectroscopic ellipsometry is the unique technique applied to study the optical properties of thick transparent films[10−13]. In terms of the conventional ellipsometry method, there are mainly two issues involved in the film data analysis procedure: (1) requirement of an initial estimate of film thickness in approximation close to the true value, and (2) the application of the optimal numerical algorithm in data analysis with minimal error. However, in the situation in which the film thickness is close to the incident light wavelength, the data analysis with the conventional ellipsometric method can result in larger error in certain conditions, because spatial effects have not been taken into account in the data analysis procedure.

A modified ellipsometric analytical method is hereby proposed to reduce the error occurring in the conventional method by taking the spatial interference effect into consideration[14]. The accuracy of the modified ellipsometric data analysis is tested and proven for the film thickness of less than 200 nm, i.e., the film thickness is less than the incident wavelength. However, for a film thicker than the wavelength, the accuracy of the modified ellipsometric analysis method has not yet been studied and reported. In this letter, we focus the ellipsometric study on the experimental condition, in which transparent film thickness is larger than the wavelength of incident light. Two samples with different thickness of SiO_2 films deposited on the Si substrate are produced using e-beam evaporation. Through the modified ellipsometric method, the error between theoretical and experimental ellipsometric data for thick film has been significantly decreased, especially under the condition where the phase delay is equal to about $m\pi$ for the integer number m ranging from 8 to 16. The results given in this work reveal that higher accuracy can be achieved with the modified ellipsometric method in the wider range of the film thickness, which can be applied to other optical measurement with the data analysis for thick film structures.

The schematic diagram of a single SiO_2layer deposited on the Si substrate is shown in Fig. 1. The light is incident at the angle θ_0 from air onto the transparent SiO_2 film with thickness d and refractive index n_1. The Si substrate has a complex refractive index of $\tilde{n}_2(\tilde{n}_2 = n_2 + ik_2$, where n_2 and k_2 are the real and imaginary parts of the index, respectively). The light propagating in the film comes out along the y direction with a phase delay of $\delta = 4\pi n_1 d(\cos\theta_1)/\lambda$, where λ is the wavelength and θ_1 is the refraction angle at the SiO_2 film side. When the light propagates from medium i to j, the light path directions at the interface of the two media obey Snell's law expressed as

$$n_i \sin\theta_i = n_j \sin\theta_j. \qquad (1)$$

In terms of multiple reflection interferences occurring in the film structure, the effective reflection coefficients for the monolayer film structure are given by[15]:

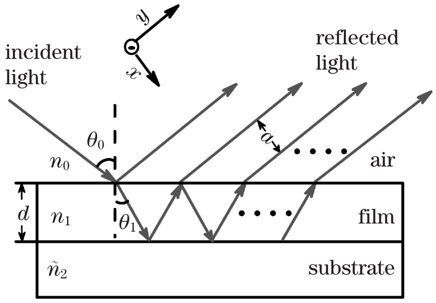

Fig. 1. Schematic diagram of the single-layer air/SiO$_2$/Si film structure with thickness d, where θ_0 and θ_1 are the incident and the refractive angles at the SiO$_2$film side, respectively; and n_0, n_1 and $\tilde{n}_2$ are the refractive indices of the medium of air, SiO$_2$ film, and Si substrate, respectively.

$$r^{\mathrm{p,s}} = r_{01}^{\mathrm{p,s}} + [1-(r_{01}^{\mathrm{p,s}})^2] r_{12}^{\mathrm{p,s}} \mathrm{e}^{-\mathrm{i}\delta} \sum_{k=2}^{\infty} (-r_{01}^{\mathrm{p,s}} r_{12}^{\mathrm{p,s}} \mathrm{e}^{-\mathrm{i}\delta})^{n-2}, \quad (2)$$

where r^{p} and r^{s} represent the reflection coefficients of the light polarized in parallel and perpendicular to the incidence plane, respectively.

The conventional ellipsometry equation is given as[16−18]

$$\frac{r^{\mathrm{p}}}{r^{\mathrm{s}}} = \tan \Psi \exp(\mathrm{i}\Delta), \quad (3)$$

where Ψ and Δ are the ellipsometric parameters as measured in the experiment. When light is incident obliquely onto the film surface, there is an actual spatial separation along the x direction between the two neighboring light beams under the condition $\theta_0 \neq 0$. Taking consideration of the spatial effect, the modified reflection coefficients of thin films $r_{\mathrm{sp}}^{\mathrm{p}}$ and $r_{\mathrm{sp}}^{\mathrm{s}}$ (the subscript sp refers to the term "spatial") can be presented as

$$r_{\mathrm{sp}}^{\mathrm{p,s}} = r_{01}^{\mathrm{p,s}} g_1 + [1-(r_{01}^{\mathrm{p,s}})^2] r_{12}^{\mathrm{p,s}} \mathrm{e}^{-\mathrm{i}\delta} \sum_{k=2}^{\infty} (-r_{01}^{\mathrm{p,s}} r_{12}^{\mathrm{p,s}} \mathrm{e}^{-\mathrm{i}\delta})^{n-2} g_k(x), \quad (4)$$

where $g_1 = \exp(-x^2/2\mathrm{w})$ is the spatial distribution of the first reflected beam, the spatial distribution parameter of $g_k(x)$ is assumed to have the Gaussian formation[19] for the multiple-reflected beams along the x direction as indicated in Fig. 1. The spatial distribution parameter of $g_k(x)$ is defined as

$$g_k(x) = \exp\{-[x-(k-1)a]^2/2w^2\}, \quad (5)$$

where k is the intger which represents serial number for the reflected beam w is the width of the wave packet in assumption, and a is the spatial separation along the x direction between the two neighboring light beams under the condition $\theta_0 \neq 0$ as shown in

$$a = \frac{d \sin(2\theta_0)}{\sqrt{n_1^2 - \sin^2\theta_0}}. \quad (6)$$

Therefore, the ellipsometric parameters in the modified model are written as[14]

$$\tan \Psi_s = \left(\frac{I_{\mathrm{sp}}^{\mathrm{p}}}{I_{\mathrm{sp}}^{\mathrm{s}}}\right)^{\frac{1}{2}}, \quad \cos \Delta_{\mathrm{s}} = \frac{I_{\mathrm{sp}}^{\mathrm{ps}}}{\left(I_{\mathrm{sp}}^{\mathrm{s}} I_{\mathrm{sp}}^{\mathrm{p}}\right)^{\frac{1}{2}}}, \quad (7)$$

where $I_{\mathrm{sp}}^{\mathrm{p,s}}$ and $I_{\mathrm{sp}}^{\mathrm{ps}}$ are the measured intensities of total reflected light for the pure p-s and cross p-s components, respectively, and are defined as

$$I_{\mathrm{sp}}^{\mathrm{p,s}} = I_{\mathrm{o}}^{\mathrm{a}} \int_{-\infty}^{\infty} [r_{\mathrm{sp}}^{\mathrm{p,s}}(x)][r_{\mathrm{sp}}^{\mathrm{p,s}}(x)]^* \mathrm{d}x,$$

$$I_{\mathrm{sp}}^{\mathrm{ps}} = I_{\mathrm{o}}^{\mathrm{a}} \int_{-\infty}^{\infty} \mathrm{Re}\left\{[r_{\mathrm{sp}}^{\mathrm{p}}(x)][r_{\mathrm{sp}}^{\mathrm{s}}(x)]^*\right\} \mathrm{d}x, \quad (8)$$

where $I_{\mathrm{o}}^{\mathrm{a}}$ is the normalized intensity of the light in the integral space.

Two SiO$_2$ films (samples A and B) deposited onto the Si substrate were produced by e-beam evaporation to study the phenomena. In order to obtain homogenous thicknesses, the SiO$_2$ films with the size of about 14 mm in diameter were evaporated under the narrow evaporation angle condition of less than 1.1° in the vacuum chamber which has a size of about 1.1 m in diameter. In order to obtain uniform film samples, the film growth rate was controlled in the constant of 10 nm/s by MDC–360 quartz oscillator (MAXTEX Inc). In the film growth process, the base pressure of the vacuum chamber was 1.8×10^{-3} Pa. By fully controlling film growth rate with the background vacuum pressure, the thick SiO$_2$ film can be considered to have a homogeneous optical constant in the film profile.

The ellipsometric parameters of Ψ and Δ were measured for the samples using the scanning ellipsometer that synchronously rotated the polarizer and analyzer[20] at 5 incidence angles (50°, 55°, 60°, 65°, and 70°) and in the 3–4.5 eV photon energy range. Data are shown in Figs. 2(a) and (b) for samples A and B, respectively. The physical fit structure used in analyzing ellipsometric parameters was substrate/sellmeier-model-layer/air. The film thickness for each sample was initially measured and controlled by the MDC–360 quartz oscillator, and the obtained values are equal to about 0.7 and 1.0 μm, respectively. The physical thicknesses of the samples were measured by ellipsometry at a 50° incident angle, and were equal to 686.03 and 977.67 nm for samples A and B, respectively. The optical refractive index n_1 of the SiO$_2$ film in the visible range changed slightly with the wavelength. Due to the uniformity of the film in the growth process, the refractive index of SiO$_2$ films did not change much with the thickness. Therefore, we used the film with a thickness of 50 nm as a standard sample to obtain the refractive index of SiO$_2$ films by analyzing its ellipsometric parameters under the condition in which the conventional ellipsometric analysis were accurate enough for the phase delay δ of less than π[14].

We define the standard mean square error (MSE) between the modeling and experiment data as

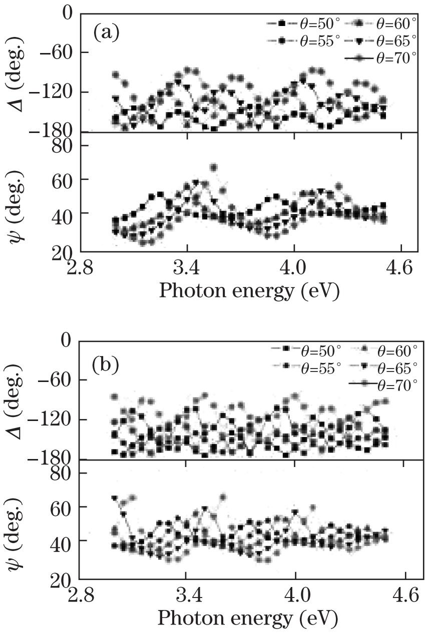

Fig. 2. Spectra of the ellipsometric parameters Ψ and Δ for the air/SiO$_2$/Si structure measured at 5 incident angles (50°, 55°, 60°, 65°, and 70°) in the 3.0–4.5 eV photon energy range with the results shown in (a) and (b) for samples A and B, respectively.

$$\mathrm{MSE}=\sqrt{\frac{1}{q}\sum_{i=1}^{q}\left[\left(\Psi_i^{\mathrm{mod}}-\Psi_i^{\mathrm{exp}}\right)^2+\left(\Delta_i^{\mathrm{mod}}-\Delta_i^{\mathrm{exp}}\right)^2\right]},\tag{9}$$

where q is the total number of experimental data set of Ψ and Δ. Thus, MSE can be used to examine the accuracy of data analysis using two ellipsometric methods.

Both Ψ^{mod} and Δ^{mod} were initially analyzed for two samples using the conventional ellipsometric Eqs. (2) and (3). The results illustrated in Fig. 3(a) show that the MSE increased with increasing film thickness and incidence angles. In terms of the modified ellipsometric Eqs. (4)–(8), the higher orders of sum ($n > 10$) can be omitted due to smaller $r_{01}^{\mathrm{p,s}}$ values at the air/SiO$_2$ interface in the 50°–70° incidence angle range. There is the uncertainty that the width of the wave packet can spread with time as the light wave propagates in space[17]. The width of wave packet $w = 7.7\lambda$ has been used in the data analysis under the assumption that all light waves approximately have the same packet size after emerging from the film structure. Therefore, using the modified ellipsometry model, the errors between the measured and analyzed data is significantly reduced as shown in Figs. 3(b) and (c) for samples A and B, respectively.

Through the square-dotted black line in Fig. 4, it has been shown that the standard error resulting from the conventional ellipsometric analysis is more significant at the region where the phase delay δ is approximately equal to $m\pi$ for the integer number m ranging from 8–16. The error has been reduced by applying the modified ellipsometry model on the data analysis. The result is shown by the circle-dotted line in Fig. 4, which corresponds to the phase delay δ changing in the ranges of 7.5–11.5 π and 10.5–16.5 π for samples A and B, respectively.

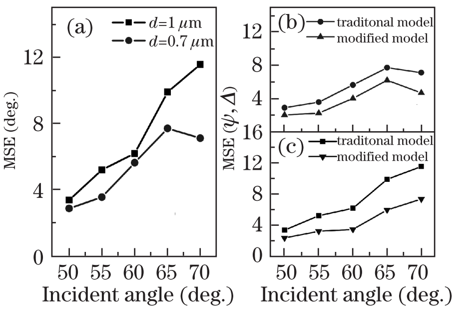

Fig. 3. Standard error (MSE) is analyzed versus incident angel in the range of 50–70° with the traditional ellipsometry models shown in (a) for samples A (round-doted line) and B (square-doted line), respectively. The standard errors (MSE) of ellipsometric parameters Ψ and Δ changing with the incident angle are compared between the traditional and modified ellipsometry model with the results shown in (b) and (c) for samples A and B, respectively.

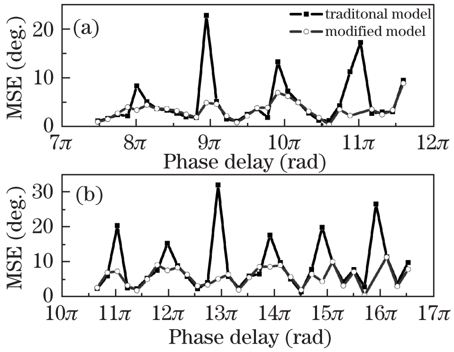

Fig. 4. Standard error (MSE) is analyzed as the function of phase delay with the results shown in (a) and (b) for samples A and B, respectively, as measured at a 70° incident angle and in the 3.3–4.5 eV incident energy range with the traditional model (square-dotted line) and the modified model (circle-dotted line).

The conventional ellipsometric analyses in Figs. 3 and 4 show that the MSE increased with increasing film thickness and incident angles and reached to local maxima at the region where the phase delay δ was approximately equal to mπ. However, using the modified ellipsometry analysis, the MSE was reduced significantly and in much closer agreement with the experiment data. Therefore, the modified ellipsometric method has higher accuracy in data analysis for the thick transparent films.

In conclusion, we use the modified ellipsometry method in data analysis to study thick transparent films. The errors arising from the conventional ellipsometric analysis increase with increasing film thickness and incident angles. In addition, we find that it periodically changes with the phase delay δ and especially showes peaks at the place where the phase delay is approximately equal to $m\pi$ for the integer number m changing from 8–16. For the transparent film, which is much thicker than the incident wavelength, the modified ellipsometric method can be used to analyze the data and reduce the error significantly, with the results in closer agreement with the experimental ones. Therefore, the results given in this letter can be applied to other optical methods to study the optical properties of the periodic or non-periodic film structures.

This work was supported by the National Natural Science Foundation of China (No. 60938004), the STCSM Project of China (No. 08DJ1400302), the Shanghai Municipal Education Commission Fund (No. 10YZ213), and the Leading Academic Discipline Project of Shanghai Municipal Education Commission (No. J5180Q).

References

1. J. Hilfiker, N. Singh, T. Tiwald, D. Convey, S. Smith, J. Baker, and H. Tompkins, Thin Solid Films **516,** 7979 (2008).
2. R. Shrestha, D. Yang, and E. Irene, Thin Solid Films **500,** 252 (2006).
3. C. Walsh and E. Franses, Thin Solid Films **347,** 167 (1999).
4. J. Rivory, Thin Solid Films **313,** 333 (1998).
5. S. Colard and M. Mihailovic, Thin Solid Films **336,** 362 (1998).
6. I. An, J. Nanophotonics **2,** 021905 (2008).
7. M. Vinodh, L. Jeurgens, and E. Mittemijer, J. Appl. Phys. **100,** 044903 (2006).
8. M. Camacho-Lopez, C. Sanchez-Perez, A. Esparza-Garcia, E. Ghibaudo, S. Rodil, S. Muhl, and L. Escobar-Alarcon, Proc. SPIE **5622,** 545 (2004).
9. H. McKay, R. Feenstra, T. Schmidtling, U. Pohl, and J. Geisz, J. Vac. Sci. Technol. B **19,** 1644 (2001).
10. S. Guo, G. Gustafsson, O. Hagel, and H. Arwin, Appl. Opt. **35,** 1693 (1996).
11. S. Bosch, J. Pérez, and A. Canillas, Appl. Opt. **37,** 1177 (1998).
12. J. Campmany, E. Bertran, A. Canillas, J. Andújar, and J. Costa, J. Opt. Soc. Am. A **10,** 713 (1993).
13. V. Odarich, J. Opt. Technol. **75,** 132 (2008).
14. M. Sheng, Y. Wu, S. Feng, Y. Chen, Y. Zheng, and L. Chen, Appl. Opt. **46,** 7049 (2007).
15. M. Klein, *Optics* (Wiley, New York, 1970).
16. R. Azzam and N. Bashara, *Ellipsometry and polarized light* (Elsevier, Amsterdam, 1985).
17. M. Yonghong, C. She, and J. Gang, Chin. Opt. Lett. **8,** (Sup) 114 (2010).
18. W. Linjun, X. Yiben, S. Hujiang, Z. Minglong, Y. Ying, and W. Lin, Chin. Opt. Lett. **2,** 308 (2004).
19. F. S. Levin, *An introduction to quantum theory* (Cambridge University Press, Cambridge, New York, 2002) chap.7.
20. L. Chen, X. Feng, Y. Su, H. Ma, and Y. Qian, Appl. Opt. **33,** 1299 (1994).